

1 **Improvement in settleability and dewaterability of waste**
2 **activated sludge by solar photocatalytic treatment in**
3 **Ag/TiO₂-coated glass tubular reactor**

4

5 Chunguang Liu ^a, Zhongfang Lei ^a, Yingnan Yang ^a, Haifeng Wang ^a, Zhenya Zhang ^{a,*}

6

7 ^a *Graduate School of Life and Environmental Sciences, University of Tsukuba, 1-1-1*

8 *Tennodai, Tsukuba, Ibaraki 305-8572, Japan*

9 ^b *Chinese Academy of Agricultural Mechanization Sciences, No.1 Beishatan*

10 *Deshengmen Wai, Beijing 100083, China*

11

12

13

14

15

16

17

18

19

20

21

22

23

*Corresponding author: Zhenya Zhang. Tel/fax.: +81 29 853 4712.

E-mail address: zhang.zhenya.fu@u.tsukuba.ac.jp (Z. Zhang).

1

2 **Abstract**

3 In this study, photocatalysis was used to improve the dewaterability and
4 settleability of waste activated sludge (WAS) by a solar photocatalytic reactor with
5 transparent Ag/TiO₂ film as photocatalyst. Specific resistance of filtration (SRF) and
6 sludge volume index (SVI) were used to evaluate WAS dewaterability and settleability,
7 respectively, and the mechanism of photocatalysis was interpreted from the changes
8 of pellets, loosely/tightly bound extracellular polymeric substances
9 (LB-EPS/TB-EPS), proteins (PN) and polysaccharides (PS) in WAS. Results showed
10 that the SRF and SVI values decreased by 86.0% and 80.0%, respectively after
11 photocatalysis treatment for 18 h. The changes of LB-EPS/TB-EPS and morphology
12 of WAS indicated that WAS was degraded in a stepwise and mild manner, in which
13 the sludge pellets were possibly converted into TB-EPS and then LB-EPS.
14 Simultaneously, LB-EPS were degraded into carbon dioxide and water by Ag/TiO₂
15 photocatalysis.

16 **Key words:** Ag/TiO₂; solar photocatalysis; waste activated sludge; dewaterability;
17 settleability

18

19 **1. Introduction**

20 Large quantities of wastewater is treated successfully by activated sludge
21 technology. Meanwhile, a lot of waste activated sludge (WAS) is produced in this
22 process. Reducing the volume and water content of the WAS is still a major concern
23 (Yuan et al., 2011). The commonly used chemical treatment methods hardly decrease
24 water content below 80%, and the volume of dewatered sludge obviously increases

1 with the addition of inorganic conditioners (Chen et al., 2001). In order to dispose
2 WAS economically and efficiently, dewatering and settling processes are essential to
3 reduce the sludge volume, which is still a bottleneck for sludge treatment (Guan et al.,
4 2012).

5 The dewatering and settling characteristics of WAS are different based on
6 wastewater sources and treatment processes. Furthermore, detailed factors that
7 influence sludge dewaterability and settleability are not yet well understood (Yu et al.,
8 2008). Extracellular polymeric substances (EPS) concentration of WAS, proteins and
9 polysaccharides content of EPS are reported to play a predominant role in sludge
10 dewaterability and settleability (Chen et al., 2001; Li & Yang, 2007). Moreover, the
11 layered theory of EPS is proposed to explicate the mechanisms of EPS impact on
12 WAS dewaterability and settleability. EPS can be divided into loosely bound
13 extracellular polymeric substances (LB-EPS), tightly bound EPS (TB-EPS) and pellet
14 (Li & Yang, 2007; Yu et al. 2008).

15 Based on the theory above, many kinds of methods have been developed to
16 improve the sludge dewaterability and settleability, including acid or alkaline
17 treatment (Devlin et al., 2011; Thapa et al., 2009), metal ions (Fe^{3+} , Ca^{2+}) addition
18 (Liu & Horn, 2012), electro-chemical treatment (Yuan et al., 2010), thermal treatment
19 (More et al., 2012), sonication (Feng et al., 2009; Saha et al., 2011), microwave (Tang
20 et al., 2010), explosive explosion shockwave (Chen & Yang, 2012), pressurised
21 electro-osmotic (Citeau et al., 2012) and biological treatment (More et al. 2010).

22 Although these technologies exhibit some enhancement effect on sludge

1 dewaterability and settleability, some problems limit their application. On the other
2 hand, photocatalytic technology may be proposed to improve sludge dewaterability
3 and settleability by degrading EPS in WAS. Moreover, it is eco-friendly compared to
4 acid or alkaline treatment, metal ions addition and electro-chemical treatment, and
5 low-energy consumption compared to thermal treatment, sonication, microwave,
6 explosive explosion shockwave, and pressurised electro-osmotic treatment. It is also a
7 low-cost method compared to other treatment methods because it uses sunlight.

8 TiO_2 photocatalytic technology, an advanced oxidation process (AOP) utilizing free
9 radicals as a primary oxidant, has been successfully applied in wastewater treatment
10 (Gaya & Abdullah, 2008). Many organics can be degraded due to its non-selective
11 oxidation capability. It is supposed that the pore water and interstitial water in WAS
12 could be released with the degradation of WAS. In addition, the odour, turbidity and
13 organics content in WAS can be decreased during the process. Two kinds of
14 photocatalytic reactors (suspended- and supported-type) can be used in the treatment of
15 WAS. Although having higher photocatalytic activity, the suspended-type TiO_2
16 photocatalysis has higher cost of post-treatment (Mozia, 2010). Due to lower
17 interaction efficiency with contaminants and higher recombination rate of
18 electron-hole, the supported-type TiO_2 photocatalysis has lower photocatalytic
19 activity (van Grieken et al., 2009). Therefore, it is promising to synthesize some novel
20 and effective immobilized photocatalysts. Ag exhibits an efficient plasmon resonance
21 effect under sunlight and plays an important role of electron-hole separation produced
22 by TiO_2 (Ma et al., 2012). Thus, several modified TiO_2 photocatalysts with Ag-doped

1 have been developed (Ji et al., 2011). However, the effect of photocatalysis on WAS
2 dewaterability and settleability has not been reported up to now.

3 The objective of this research is to synthesize a novel Ag/TiO₂ immobilized as
4 photocatalyst which can be used under sunlight irradiation to improve WAS
5 dewaterability and settleability. The changes of LB-EPS, TB-EPS, proteins (PN) and
6 polysaccharides (PS) in WAS have been investigated during the photocatalytic
7 process in addition to their effects on specific resistance of filtration (SRF) and sludge
8 volume index (SVI) values. In addition, the variation of morphology was compared
9 between the WAS samples before and after photocatalysis by scanning Electron
10 Microscopy (SEM). The related mechanisms, especially the role of EPS in WAS
11 dewaterability and settleability are also discussed.

12 **2. Methods**

13 *2.1. WAS and catalyst*

14 The WAS was collected from a domestic wastewater treatment plant in Shimodate,
15 Ibaraki, Japan. The sludge sample was immediately transferred to the lab and stored
16 in a plastic container at 4° for use. The initial characteristics of WAS were as follows
17 (g/l except pH): pH 6.7, total solid (TS) 4.0, volatile suspended solid (VSS) 3.6, total
18 and soluble chemical oxygen demand (TCOD and SCOD) 8.7 and 0.31, respectively.

19 The catalysts used in this study were TiO₂ (control, main characteristics, bought
20 from which company, country) and Ag/TiO₂ film coated on the inner wall of
21 glass-tube, respectively. The catalyst of Ag/TiO₂ was synthesized using a modified
22 impregnation–precipitation–photoreduction method (Ma et al., 2012). Briefly, the

1 TiO₂-film coated glass tubes were impregnated by immersing into AgNO₃ (which
2 company, country?) solution (0.5 mol/l) for 20 min with UV light irradiation; then the
3 glass tubes were calcined (300°C, 1 h) in a vacuum oven (Hasuc, Shanghai, China);
4 and finally, cooled to room temperature under UV-light. The phase composition and
5 the degree of crystallinity in TiO₂ and Ag/TiO₂ were determined by X-ray diffraction
6 (XRD). The XRD patterns of the as-prepared samples (2θ ranges from 10° to 90°)
7 were recorded at room temperature with scanning speed of 10° min⁻¹ using Cu Kα
8 radiation (λ= 0.154 Å) from a 40 kV X-ray source (Bruker D8 Advance).

9 2.2. *Experimental set-up*

10 All the experiments were carried out in a solar photocatalytic reactor with support
11 catalyst (shown in Fig.1), which contained 10 glass tubes (18cm in length, 1 cm in
12 diameter) with TiO₂ or Ag/TiO₂ film coated on inside wall. The working volume of
13 the reactor was 700 ml, and the WAS flowed in the reactor at 100 ml/min by a
14 peristaltic pump (??Which company, country). In this study, sunlight was used as light
15 source, and the mean UV-light intensity (290 nm – 390 nm) in sunlight was recorded
16 from 9:00 to 15:00 (shown in Fig.2(a)). The control experiments were conducted by
17 using the same reactor under the same light conditions but without catalyst on the
18 inner wall of the glass tubes.

19 2.3. *Experimental procedure*

20 The WAS was treated in the solar photocatalytic reactor for 48 h (6 h photocatalysis
21 for one day under the sunlight, then the reactor was covered with a black cloth
22 avoiding sunshine) during September 2012. Sampling was done right after

1 photocatalysis every day for subsequent analysis. Specific resistance of filtration
2 (SRF) and sludge volume index (SVI) were checked to assess the dewaterability and
3 settleability of the WAS before and after photocatalysis. LB-EPS, TB-EPS, PN and PS
4 concentrations of the sludge samples were also measured to disclose the mechanisms
5 related with the changes of sludge dewaterability and settleability.

6 *2.4. EPS extraction*

7 LB-EPS and TB-EPS were extracted from WAS by a modified heat extraction
8 method (Li & Yang, 2007). The WAS was first centrifuged (MX-301, TMY) at 4000 g
9 for 5 min in a 15-ml centrifuge tube to dewater, then the sludge sediment in the
10 centrifuge tube was re-suspended with NaCl solution (0.05%, 70°C) to the original
11 volume. Without any delay, the sludge suspension was sheared by a vortex mixer
12 (VORTEX-GENIE G-560, scientific industries, INC.) for 2 min, followed by
13 centrifugation at 4000 g for 10 min. The organic matter in the supernatant was the
14 LB-EPS of WAS. For the TB-EPS, the WAS was firstly centrifuged at 4000 g for 5
15 min in a 15-ml centrifuge tube, then the liquid phase was discarded and the solid
16 phase was re-suspended with 0.05% NaCl solution to its original volume of 15 ml.
17 Secondly, the WAS suspension was heated to 60°C (confirm this temperature, 70?) for
18 30 min in an incubator (WFO-700, EYL4). Finally, the re-suspension was centrifuged
19 (MX-301, TMY) at 4000 g for 15 min and the supernatant was collected for TB-EPS
20 analysis. The residue in the centrifuge cube was again re-suspended by adding NaCl
21 solution (0.05%, 70°C) to the original volume of 15 ml. This fraction was the pellet.

22 *2.5. Indices and analytical methods*

1 The photocatalytic activity of the TiO₂ and Ag/TiO₂ was assessed by the
2 degradation rate of methyl orange (company name, country). The changes of WAS
3 dewaterability and settleability were assessed based on the specific resistance of
4 filtration (SRF) and sludge volume index (SVI), respectively before and after
5 treatment. The SRF was measured using a slightly modified method of Li & Yang
6 (2007). The SRF(cm/g) of the sludge was calculated by
7
$$SRF = 2 \cdot b \cdot p \cdot A^2 / (\mu C)$$

8 where p (60 kPa) is the pressure applied, A ($3.0 \times 10^{-4} \text{ m}^2$) is the filter area, μ (1.0mPa s)
9 is the viscosity of the permeate, C is the sludge concentration in mixed liquor
10 suspended solids (MLSS,kg/m³) and b (s/m⁶) is the time-to-filtration ratio, which is
11 the slope of the curve obtained by plotting the ratio of the time of filtration to the
12 volume of filtrate (t/V) versus the filtrate volume (V).

13 The SVI value of WAS was obtained by measuring the sludge volume change in a
14 100-ml cylinder (100ml, ARROW) after 30 min settlement together with MLSS
15 concentration.

16 The morphology of untreated or photocatalysis treated WAS was obtained by
17 scanning electronic microscope (SEM, XL30, Philips, Holland). EPS (LB-EPS and
18 TB-EPS) concentrations were analyzed for COD, proteins (PN) and polysaccharides
19 (PS). COD and MLSS were detected in accordance with the standard methods
20 (Pawlowski, 1994). Phenol sulfuric method (Mecozzi, 2005) with glucose as standard
21 and Lowry method (Dawson & Heatlie, 1984) with bovine serum albumin as standard
22 were used to determine the concentrations of PS and PN, respectively.

1 **3. Results and discussion**

2 *3.1. Characterization and photocatalytic capacity of TiO₂ and Ag/TiO₂*

3 The XRD patterns of pure TiO₂ (1) and Ag/TiO₂ (2) samples are shown in
4 supplementary Fig.S1(a). The XRD patterns indicate that anatase is the only
5 crystalline phase of TiO₂ in the pure TiO₂ sample. The presence of Ag diffraction lines
6 (peaks marked by arrowhead in supplementary Fig.S1(a)) was clearly detected at
7 approximately 22.55° (2θ) for the Ag/TiO₂ sample.

8 The photocatalytic activity of TiO₂ and Ag/TiO₂ was assessed by the degradation of
9 methyl orange (MO, 20 mg/l) under the sunlight for 2 h from 11:00 to 13:00. The
10 UV-intensity (290 nm – 390 nm) is shown in Fig.2(b) and the degradation rate of MO
11 is shown in supplementary Fig.S1(b). It was found that Ag/TiO₂ exhibited much
12 higher MO degradation rate (99.0%) than pure TiO₂ (35.2%), and the MO degradation
13 could be negligible under single sunlight condition. This observation indicates that
14 Ag/TiO₂ possesses better photocatalytic activity than pure TiO₂. The improvement is
15 probably owing to the Ag particles deposited on the TiO₂ acting as electron–hole
16 separation and interfacial charge transfer (van Grieken et al., 2009). The charge
17 separation resulted from the formation of Schottky barriers at the Ag/TiO₂ interaction
18 region is attributable to the electron transfer from the TiO₂ conduction band to silver
19 particles (van Grieken et al., 2009). Due to the fact that the trapping of electrons by
20 Ag deposits is faster than its recombination with holes (Krejčíková et al., 2012), the
21 silver deposits on the surface can accelerate the transfer of trapped electrons in the Ag
22 deposits to the oxygen molecules to form superoxide radicals in solution and then

1 improve the photocatalytic activity (Pulido Melián et al., 2012). Because of having
2 higher photocatalytic activity than TiO_2 , Ag/TiO_2 was chosen as photocatalyst in the
3 following experiments.

4 *3.2. Effect of Ag/TiO_2 photocatalytic treatment on sludge dewaterability*

5 The effect of Ag/TiO_2 photocatalytic treatment on sludge dewaterability was
6 evaluated by measuring SRF value (Fig.3a). It can be seen that the sludge
7 dewaterability could be greatly enhanced after Ag/TiO_2 photocatalytic treatment for 18
8 h. Further prolonging the photocatalysis duration has little enhancement effect. The
9 SRF value decreased from 2.42×10^9 cm/g (untreated WAS) to 3.4×10^8 , 3.83×10^8 and
10 4.7×10^8 cm/g after photocatalytic treatment for 18 h, 24 h and 36 h, respectively.
11 Therefore, in this study, 18 h was chosen as the optimal photocatalysis time, under
12 which the SRF value could be reduced by 86.0%.

13 The above effect of photocatalysis on sludge dewaterability can be explained as
14 follows. The flocs of WAS are in layered structure (Nguyen et al., 2008), in which the
15 loose surface layer can be first damaged and dispersed into the aqueous solution and
16 then quickly oxidized into carbon dioxide by photocatalysis within a few hours. Later
17 the free water, pore water and some bound water are released resulting in rapid
18 decrease in SRF value. With the degradation of the loose surface layer, the highly
19 porous sludge flocs can become compacted spheroidal structure thus the flocs density
20 increases, which further improve the dewaterability of WAS (Jin et al., 2003). Along
21 with the photocatalysis process, the spheroidal structure of flocs is disrupted and EPS
22 is released gradually. Simultaneously, the released EPS can be degraded by Ag/TiO_2

1 photocatalysis, which may contribute to the fluctuation of SRF values during the 24
2 and 48 h treatment. This observation is in some agreement with the finding of Feng et
3 al. (2009) who treated WAS by ultrasound conditioning and pointed out that sludge
4 dewaterability could be slightly enhanced at low specific energy dosages while
5 significantly deteriorated at larger specific energy dosages (>4400 kJ/kg TS).

6 *3.3. Effect of Ag/TiO₂ photocatalytic treatment on sludge settleability*

7 The settleability, indicated by SVI, is an important factor influencing the operation
8 of sewage treatment plant. The change of SVI values is shown in Fig.3(b). Clearly, the
9 SVI decreased quickly from 161.4 ml/g to 86.7 ml/g and 58.7 ml/g after
10 photocatalysis for 12 h and 18 h, and increased slightly to 69.4 ml/g at 36 h,
11 respectively. On the other hand, the SVI value of the untreated WAS (control)
12 fluctuated between 159.1 ml/g and 172.1 ml/g during the 48 h photocatalysis
13 treatment. After 18 h photocatalysis treatment, the sludge settleability was comparable
14 to that of thermophilic aerobic granular biomass (SVI = 60 ml/g) (Zitomer et al.,
15 2007).

16 As it is known, the WAS has high SVI value due to some unfavorable operation
17 conditions resulting in slowly settleable large flocs (supplementary Fig.S2(a)).
18 However, the loose surface of flocs can be changed by Ag/TiO₂ photocatalysis as the
19 reaction progresses. The flocs become compact granule-like structure and the surface
20 roughness reduces, and then the frictional resistance between flocs begins to decline
21 during the settlement process. When the flocs are severely destructed and the EPS are
22 released gradually, the sludge density become smaller and the particles surface area

1 become larger resulting in increased buoyancy force, ultimately leading to a slight
2 increase in SVI value (Jin et al., 2003). Meanwhile, the released EPS may be
3 degraded by Ag/TiO₂ photocatalysis subsequently. That is, the concentration of EPS
4 could have some contribution to the fluctuation of SVI values between the 24 h and
5 48 h photocatalysis.

6 *3.4. Changes of EPS, PN and PS concentrations in WAS during Ag/TiO₂* 7 *photocatalysis process*

8 *3.4.1 Changes of LB-EPS, PN and PS concentrations in WAS*

9 The changes in LB-EPS (expressed in COD), PN and PS concentrations of the
10 WAS are shown in Fig.4. The concentrations of LB-EPS and PN in LB-EPS
11 (LB-EPS/PN) declined from the initial 364.0 mg/l and 248.2 mg/l to 210.8 mg/l and
12 164.3 mg/l at 18 h, and increased to 269.1 mg/l and 221.0 mg/l at 24 h, and then
13 decreased to 220.6 mg/l and 182.7 mg/l at 36 h, respectively. However, the
14 concentrations of LB-EPS and LB-EPS/PN increased to 439.5 mg/l and 306.5 mg/l at
15 48 h, respectively. On the other hand, the concentration of PS in LB-EPS (LB-EPS/PS)
16 decreased from the start to the end of the Ag/TiO₂ photocatalytic treatment. When the
17 SRF and SVI reached the minimal values after 18 h photocatalysis yielding its
18 maximum dewaterability and settability, the LB-EPS concentration in the treated
19 sludge was 210.8 mg/l (Figs.3 and 4), less than the result (400-500mg/l) obtained by
20 Feng et al. (2009). Moreover, during the first 36 h duration of Ag/TiO₂ photocatalysis,
21 LB-EPS concentration was found to have a similar change tendency with the SRF and
22 SVI values of the sludge (Figs.3 and 4).

1 The above phenomena can be interpreted as that the widely dispersed LB-EPS in
2 the aqueous phase has more chance to interact with the photocatalyst, possibly leading
3 to its rapid degradation into carbon dioxide. With the degradation of LB-EPS, an
4 abundant amount of bound water is released, resulting in the decrease of SRF and SVI
5 values. The main components of LB-EPS are PN and PS, and the concentration of PN
6 is much higher than that of PS (Yu et al., 2008), which may be the reason why PN
7 concentration changed in a similar tendency as LB-EPS did. When the sludge flocs
8 are destroyed further by Ag/TiO₂ photocatalysis, more EPS and cellular substances
9 can be released into the aqueous phase, bringing about the increase in protein and
10 polysaccharide levels. On the other hand, EPS may be released from the pellets of
11 WAS along with its degradation. That is, the degradation and release rate of LB-EPS
12 in WAS dominates the SVI and SRF values.

13 *3.4.2 Changes of TB-EPS, PN and PS concentrations in WAS*

14 During the first 12 h photocatalysis, the concentrations of TB-EPS and PN in
15 TB-EPS (TB-EPS/PN) decreased slightly from 470.8 mg/l and 430.0 mg/l , and their
16 concentrations varied with the same tendency as the SVI and SRF values of WAS (Fig.
17 4). After that the concentrations of TB-EPS and TB-EPS/PN increased significantly
18 till the 24 h, and then decreased. This observation is inconsistent with the variation of
19 SVI and SRF values (Figs. 3 and 4). Still the concentration of PS in TB-EPS
20 (TB-EPS/PS) decreased gradually during the whole photocatalysis process.

21 The reduction of TB-EPS in the initial phase is probably due to the conversion of
22 TB-EPS to LB-EPS by Ag/TiO₂ photocatalysis, and during this period the WAS

1 pellets haven't been disrupted into TB-EPS or LB-EPS. With the photocatalysis going
2 on, the pellets are disrupted, and then more and more LB-EPS and TB-EPS are
3 released, leading to the increase of TB-EPS in WAS. Simultaneously, the increase of
4 TB-EPS can supply more LB-EPS. When the increasing portion of TB-EPS is more
5 than its decreasing counterpart, the concentration of TB-EPS will increase and vice
6 versa. However, no direct correlation has been found between TB-EPS and the SVI or
7 SRF value in this study. LB-EPS content appears to have a closer correlation with the
8 sludge characteristics in settleability and dewaterability than the TB-EPS, which
9 agrees with the finding of Yuan et al. (2011). Detailed and followed-up research is
10 necessary.

11 *3.5. Effect of Ag/TiO₂ photocatalytic treatment on the morphological change of WAS*

12 The morphological change between untreated and photocatalysis treated WAS
13 samples is obvious (supplementary Fig.S2). From the direct observation as shown in
14 supplementary Fig.S2(a), the color of sludge was changed from the original dark-gray
15 to the earth-yellow, and the concentration of flocs in WAS decreased after treatment
16 by Ag/TiO₂ photocatalysis. In addition, the obvious difference in the microstructures
17 of WAS could be observed by SEM. The surface of untreated WAS sample
18 (supplementary Fig.S2(b)) had a relatively rough surface and layered structure, while
19 the surface of photocatalysis treated WAS (after 18 h treatment) became level and
20 smooth (supplementary Fig.S2 (c)). This morphological change indicates that the
21 WAS could be degraded gradually by Ag/TiO₂ photocatalysis. When the flocs in WAS
22 are gradually degraded from surface to inside, free water and pore water can be

1 released and the frictional resistance between flocs decreases, which may contribute
2 to the decrease of SRF and SVI values. This mechanism is different from other sludge
3 treatment methods such as explosive explosion shockwave, microwave and ultrasonic
4 processes characterized as rapid and violent (Chen & Yang, 2012; Feng et al., 2009;
5 Tang et al., 2010). The appearance of photocatalysis treated WAS (for 36 h) became
6 rough, fluffy and irregularly shaped again, but not the layered structure as before
7 (supplementary Fig.S2 (d)). This observation indicates that the sludge flocs might be
8 broken, and the intracellular substances could be solubilized into the aqueous phase,
9 leading to the increase of EPS. Meanwhile, some of the EPS, especially LB-EPS, can
10 be degraded by Ag/TiO₂ photocatalysis (shown in Fig.4 (a)). So the physically bound
11 water and interstitial cell water can be released into the solution during the
12 degradation progress of EPS, enhancing sludge dewaterability and settleability.

13 **4. Conclusions**

14 A photocatalyst of Ag/TiO₂ film was synthesized and immobilized successfully, and
15 its photocatalytic activity was significantly higher than TiO₂ film. The effect of
16 Ag/TiO₂ photocatalysis on WAS dewaterability and settleability was dependent on
17 photocatalytic time. The optimal photocatalytic time was 18 h with Ag/TiO₂ as
18 photocatalyst, and the SRF and SVI values were reduced by 86.0% and 80.0%,
19 respectively. The LB-EPS and PN had more positive relation with SRF and SVI
20 during the first 36 h photocatalysis. The EPS change and SEM images of WAS
21 indicated that WAS were degraded by Ag/TiO₂ photocatalysis in a stepwise and mild
22 manner.

1 **Acknowledgements**

2 The authors are grateful to Ms. Yingxin Zhao (Graduate School of Life and
3 Environmental Sciences, the University of Tsukuba) for her help with a part of the
4 experiments. The authors also appreciate Ms. Huiling Zhang (Chinese Language &
5 Culture College, the Beijing Normal University) for providing language help and
6 writing assistance.

7 **Supplementary data**

8 The supplementary data associated with this article included Fig.S1 (XRD patterns
9 and photocatalytic activity of pure TiO₂ and Ag/TiO₂) and Fig.S2 (morphological
10 changes of WAS).

11 **References**

- 12 1. Chen, D., Yang, J. 2012. Effects of explosive explosion shockwave pretreatment
13 on sludge dewaterability. *Bioresour. Technol.* 119, 35-40.
- 14 2. Chen, Y., Yang, H., Gu, G. 2001. Effect of acid and surfactant treatment on
15 activated sludge dewatering and settling. *Water Res.* 35, 2615-2620.
- 16 3. Citeau, M., Olivier, J., Mahmoud, A., Vaxelaire, J., Larue, O., Vorobiev, E. 2012.
17 Pressurised electro-osmotic dewatering of activated and anaerobically digested
18 sludges: Electrical variables analysis. *Water Res.* 46, 4405-4416.
- 19 4. Dawson, J.M., Heatlie, P.L. 1984. Lowry method of protein quantification:
20 Evidence for photosensitivity. *Anal. Biochem.* 140, 391-393.
- 21 5. Devlin, D.C., Esteves, S.R.R., Dinsdale, R.M., Guwy, A.J. 2011. The effect of
22 acid pretreatment on the anaerobic digestion and dewatering of waste activated

- 1 sludge. *Bioresour. Technol.* 102, 4076-4082.
- 2 6. Feng, X., Deng, J., Lei, H., Bai, T., Fan, Q., Li, Z. 2009. Dewaterability of waste
3 activated sludge with ultrasound conditioning. *Bioresour. Technol.* 100,
4 1074-1081.
- 5 7. Gaya, U.I., Abdullah, A.H. 2008. Heterogeneous photocatalytic degradation of
6 organic contaminants over titanium dioxide: A review of fundamentals, progress
7 and problems. *J. Photoch. Photobio C- Photoch. rev.* 9, 1-12.
- 8 8. Guan, B., Yu, J., Fu, H., Guo, M., Xu, X. 2012. Improvement of activated sludge
9 dewaterability by mild thermal treatment in CaCl₂ solution. *Water Res.* 46,
10 425-432.
- 11 9. Ji, Z., Ismail, M.N., Callahan Jr, D.M., Pandowo, E., Cai, Z., Goodrich, T.L.,
12 Ziemer, K.S., Warzywoda, J., Sacco Jr, A. 2011. The role of silver nanoparticles
13 on silver modified titanosilicate ETS-10 in visible light photocatalysis. *Appl.*
14 *Catal. B- Environ.* 102, 323-333.
- 15 10. Jin, B., Wilén, B.-M., Lant, P. 2003. A comprehensive insight into floc
16 characteristics and their impact on compressibility and settleability of activated
17 sludge. *Chem. Eng. J.*, 95, 221-234.
- 18 11. Krejčíková, S., Matějová, L., Kočí, K., Obalová, L., Matěj, Z., Čapek, L.,
19 Šolcová, O. 2012. Preparation and characterization of Ag-doped crystalline titania
20 for photocatalysis applications. *Appl. Catal. B- Environ.* 111–112, 119-125.
- 21 12. Li, X.Y., Yang, S.F. 2007. Influence of loosely bound extracellular polymeric
22 substances (EPS) on the flocculation, sedimentation and dewaterability of

- 1 activated sludge. *Water Res.* 41, 1022-1030.
- 2 13. Liu, C., Yang, Y., Wang, Q., Kim, M., Zhu, Q., Li, D., Zhang, Z. 2012a.
- 3 Photocatalytic degradation of waste activated sludge using a circulating bed
- 4 photocatalytic reactor for improving biohydrogen production. *Bioresour. Technol.*
- 5 125, 30-36.
- 6 14. Liu, F., Zhou, L., Zhou, J., Song, X., Wang, D. 2012b. Improvement of sludge
- 7 dewaterability and removal of sludge-borne metals by bioleaching at optimum pH.
- 8 *J. Hazard. Mater.* 221–222, 170-177.
- 9 15. Liu, S., Horn, H. 2012. Effects of Fe(II) and Fe(III) on the single-stage
- 10 deammonification process treating high-strength reject water from sludge
- 11 dewatering. *Bioresour. Technol.* 114, 12-19.
- 12 16. Ma, B., Guo, J., Dai, W.-L., Fan, K. 2012. Ag-AgCl/WO₃ hollow sphere with
- 13 flower-like structure and superior visible photocatalytic activity. *Appl. Catal. B-*
- 14 *Environ.* 123–124, 193-199.
- 15 17. Mecozzi, M. 2005. Estimation of total carbohydrate amount in environmental
- 16 samples by the phenol–sulphuric acid method assisted by multivariate calibration.
- 17 *Chemometr. Intell. Lab.* 79, 84-90.
- 18 18. More, T.T., Yan, S., Hoang, N.V., Tyagi, R.D., Surampalli, R.Y. 2012. Bacterial
- 19 polymer production using pre-treated sludge as raw material and its flocculation
- 20 and dewatering potential. *Bioresour. Technol.* 121, 425-431.
- 21 19. More, T.T., Yan, S., Tyagi, R.D., Surampalli, R.Y. 2010. Potential use of
- 22 filamentous fungi for wastewater sludge treatment. *Bioresour. Technol.* 101,

- 1 7691-7700.
- 2 20. Mozia, S. 2010. Photocatalytic membrane reactors (PMRs) in water and
3 wastewater treatment. A review. *Sep. Purif. Technol.* 73, 71-91.
- 4 21. Nguyen, T.P., Hilal, N., Hankins, N.P., Novak, J.T. 2008. The relationship
5 between cation ions and polysaccharide on the floc formation of synthetic and
6 activated sludge. *Desalination* 227, 94-102.
- 7 22. Pawlowski, L. 1994. Standard methods for the examination of water and
8 wastewater, 18th edition: Arnold E. Greenberd, Lenore S. Clesceri, Andrew D.
9 Eaton (Editors) Water Environment Federation, Alexandria, USA, 1992; 1025 pp;
10 ISBN 0-87553-207-1. *Science of The Total Environment*, 14, 227-228.(confirm?)
- 11 23. Pulido Melián, E., González Díaz, O., Doña Rodríguez, J.M., Colón, G., Navío,
12 J.A., Macías, M., Pérez Peña, J. 2012. Effect of deposition of silver on structural
13 characteristics and photoactivity of TiO₂-based photocatalysts. *Appl. Catal. B-
14 Environ.* 127, 112-120.
- 15 24. Saha, M., Eskicioglu, C., Marin, J. 2011. Microwave, ultrasonic and
16 chemo-mechanical pretreatments for enhancing methane potential of pulp mill
17 wastewater treatment sludge. *Bioresour. Technol.* 102, 7815-7826.
- 18 25. Schuler, A.J., Jang, H. 2007. Microsphere addition for the study of biomass
19 properties and density effects on settleability in biological wastewater treatment
20 systems. *Water Res.* 41, 2163-2170.
- 21 26. Tang, B., Yu, L., Huang, S., Luo, J., Zhuo, Y. 2010. Energy efficiency of
22 pre-treating excess sewage sludge with microwave irradiation. *Bioresour. Technol.*

- 1 101, 5092-5097.
- 2 27. Thapa, K.B., Qi, Y., Clayton, S.A., Hoadley, A.F.A. 2009. Lignite aided
3 dewatering of digested sewage sludge. *Water Res.* 43, 623-634.
- 4 28. van Grieken, R., Marugán, J., Sordo, C., Martínez, P., Pablos, C. 2009.
5 Photocatalytic inactivation of bacteria in water using suspended and immobilized
6 silver-TiO₂. *Appl. Catal. B- Environ.* 93, 112-118.
- 7 29. Yu, G.-H., He, P.-J., Shao, L.-M., He, P.-P. 2008a. Stratification Structure of
8 Sludge Floccs with Implications to Dewaterability. *Environ. Sci. Technol.* 42,
9 7944-7949.
- 10 30. Yu, G.-H., He, P.-J., Shao, L.-M., Zhu, Y.-S. 2008b. Extracellular proteins,
11 polysaccharides and enzymes impact on sludge aerobic digestion after ultrasonic
12 pretreatment. *Water Res.* 42, 1925-1934.
- 13 31. Yuan, H.-p., Cheng, X.-b., Chen, S.-p., Zhu, N.-w., Zhou, Z.-y. 2011. New sludge
14 pretreatment method to improve dewaterability of waste activated sludge.
15 *Bioresour. Technol.* 102, 5659-5664.
- 16 32. Yuan, H., Zhu, N., Song, L. 2010. Conditioning of sewage sludge with
17 electrolysis: Effectiveness and optimizing study to improve dewaterability.
18 *Bioresour. Technol.* 101, 4285-4290
- 19 33. Zitomer, D.H., Duran, M., Albert, R., Guven, E. 2007. Thermophilic aerobic
20 granular biomass for enhanced settleability. *Water Res.* 41, 819-825.
- 21

1 Figure captions

2 Fig.1. Schematic of Ag/TiO₂-coated glass tubular photocatalytic reactor.

3 Fig.2. UV-light mean intensity used in WAS treatment (a) and used in methyl orange
4 treatment (b).

5 Fig.3. Effect of Ag/TiO₂ photocatalytic treatment on sludge dewaterability (a) and
6 settleability (b).

7 Fig.4. Changes of LB-EPS and TB-EPS concentrations in WAS during the Ag/TiO₂
8 photocatalysis process (a); Changes of PN and PS in LB-EPS and TB-EPS during the
9 Ag/TiO₂ photocatalysis process (b).

10

11

12

13

14

15

16

17

18

19

20

21

22

23

24

25

26

27

28

29

30

31

32

33

34

1
2
3
4
5
6
7
8
9
10
11
12
13
14
15
16
17
18
19
20
21
22
23
24
25
26
27
28
29
30
31
32
33
34
35
36
37
38
39
40
41
42
43
44

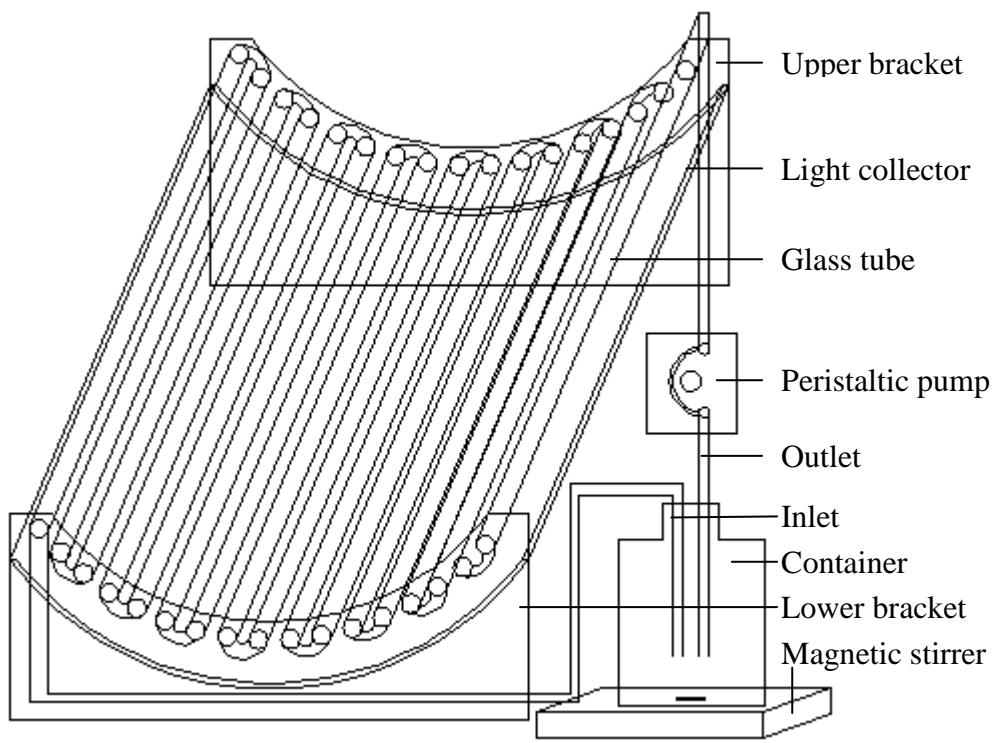
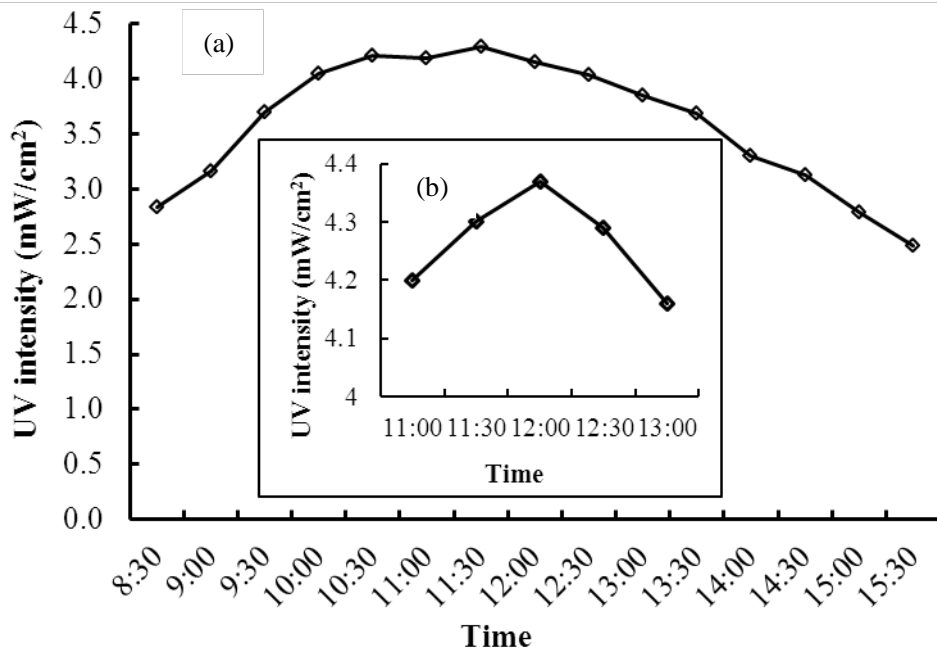
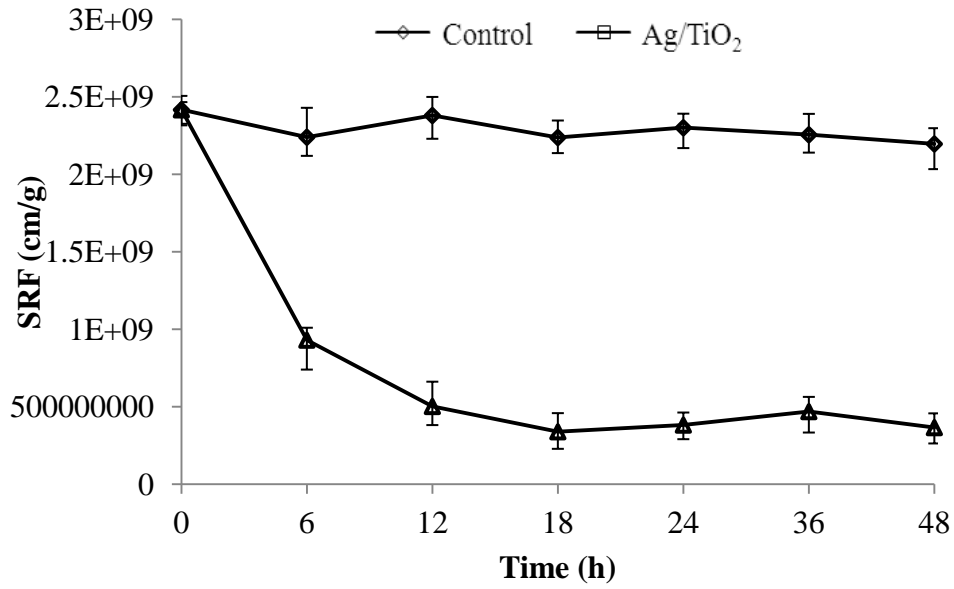


Fig.1. Liu et al.



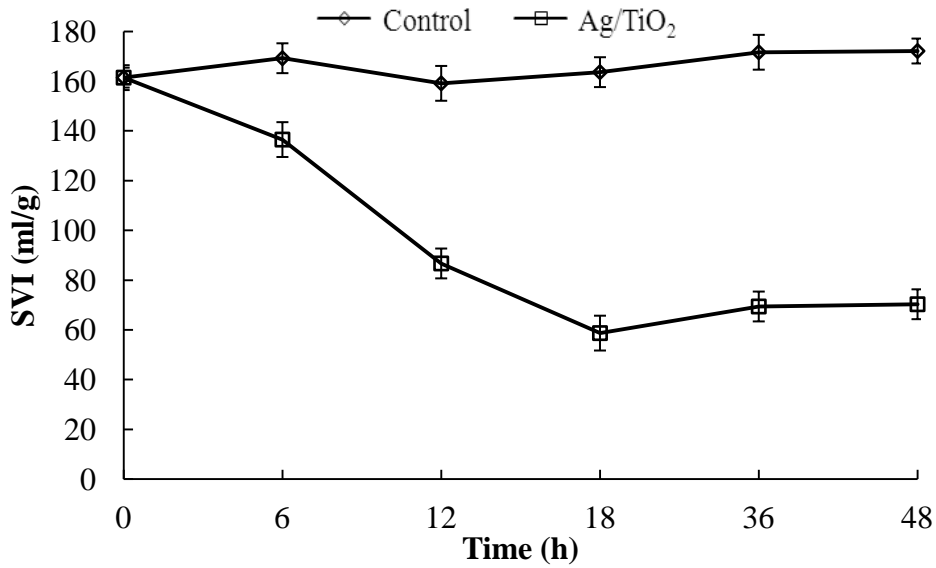
1
2
3
4
5
6
7
8
9
10
11
12
13
14
15
16
17
18
19
20
21
22
23
24
25
26

Fig.2. Liu et al.



1
2
3

Fig.3(a). Liu et al.



4
5
6
7
8
9
10
11
12
13
14

Fig.3(b). Liu et al.

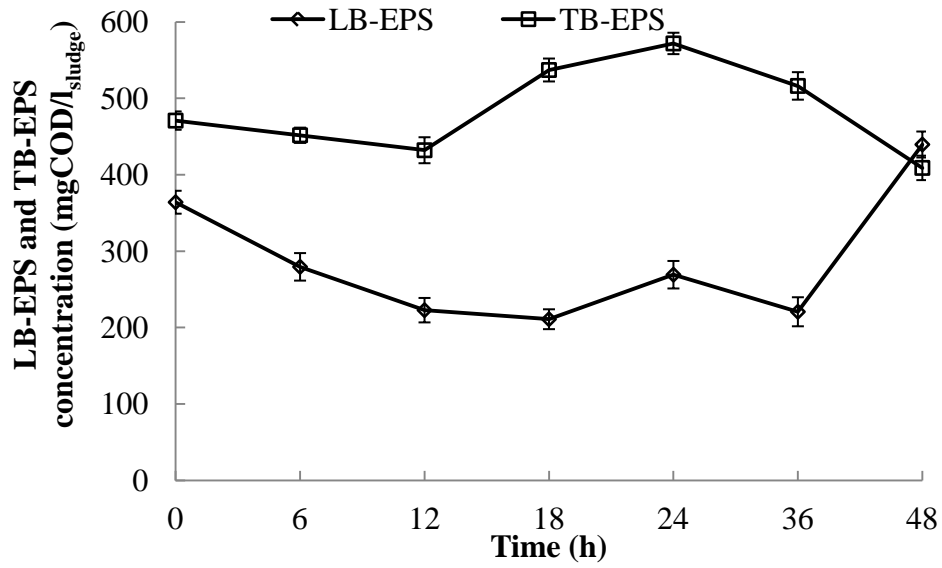


Fig.4(a). Liu et al.

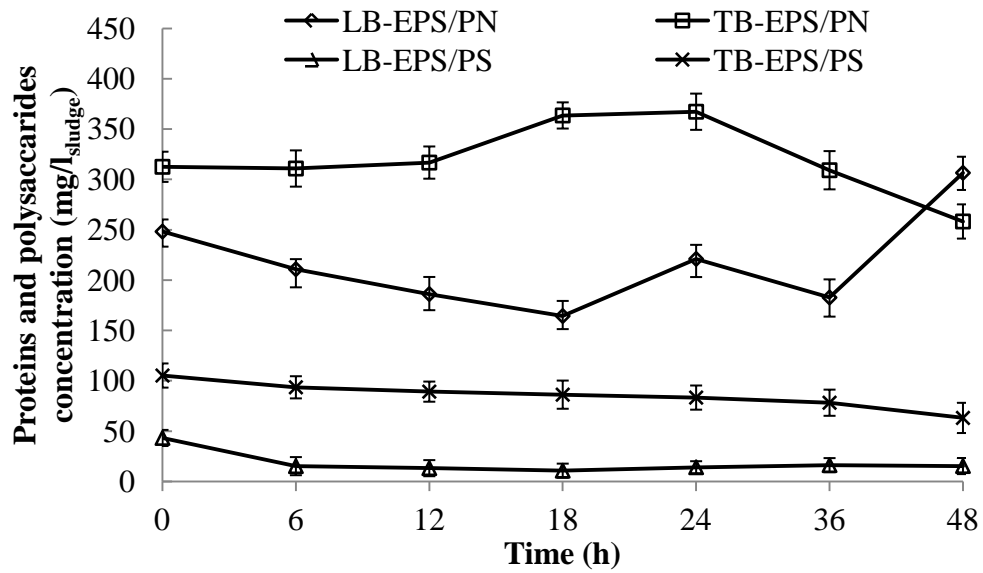


Fig.4(b). Liu et al.

1

2

3

4

5

6

7